

COMPUTATIONAL DESIGN OF FIBRE NETWORK BY DISCRETE ELEMENT METHOD

*Shakhawath Hossain, Per Bergström, Sohan Sarangi
and Tetsu Uesaka*

Department of Chemical Engineering and FSCN, Mid Sweden University,
Sundsvall, Sweden

ABSTRACT

Soft fibre networks, typically seen in bathroom tissues, kitchen towels, and personal-care products, have properties that are intricately affected by the details of fibre geometry, 3D-network structures, and processing conditions. Designing such materials and products for better performance, while controlling cost, is especially a challenge in today's fast-paced product development. This paper concerns the development of a new, robust computational design platform for the design of soft fibre networks.

We have used particle-based methods, particularly, Discrete Element Method (DEM), to model fibres, fibre networks, their properties and performance, and also unit processes for manufacturing. Unlike other computational methods, this method has advantages to model discrete and non-homogeneous materials, complex geometries, and highly non-linear dynamic problems, such as large deformation (flow), contact/non/contact, fracture, and fragmentation.

With this approach, fibres are represented by a series of connected spherical particles in different lengths and geometries (curl, kinks, twists). Fibre networks are created by the deposition of those fibres under gravity, followed by the subsequent consolidation under pressure. These processes have shown an interesting transition phenomenon from a highly fluidic granular system to a fragile soft solid. The

network is then subjected to a creping process, a critical process of tissue-making. The model was able, not only to reproduce unique crepe frequencies, but also unprecedented details of the destruction of fibre network structures and fibre failure (dusting) during creping. Typical tensile tests, thickness-direction compression tests, and softness tests have been also performed to demonstrate unique deformation characteristics of low-density, low-basis weight fibre networks.

This computational design system based on DEM provides a promising platform for exploring large parameter space of new material/product design.

1. INTRODUCTION

This paper concerns the design of fibre networks, especially for hygiene products, such as bathroom tissue, kitchen towel, baby diapers, and incontinence- and feminine-care products. For these “soft papers”, their primary performance is tactile properties, for example, softness, resilience, pliability, wicking, and structural integrity. These properties are intricately related to the selection of fibres, chemical additives, their formulations, and, of course, process conditions [34].

Traditionally, designing materials and products has been often done by starting from materials and processes and then investigating their effects on properties and performance (the cause-to-effect paradigm in Figure 1). This approach normally requires iteration to find an optimum condition for performance and cost, and thus massive trials in laboratory, pilot plant, or production mill. It is, however, becoming increasingly difficult in today’s fast-paced product development. In addition, because of its empirical nature, it is difficult to obtain deep understanding and insights for innovative design solutions. Today, materials/product design actually starts from performance goals, and then proceeds to find out specific materials, structures and process conditions that achieve the performance target at the minimum cost (the goal-to-means paradigm in Figure 1). It is an *inverse* problem, requiring a different approach. Computational material design, which have been evolved steadily for the last two decades, have great potential to innovate product development processes in the new paradigm [1].

From the computational design view point, a unique problem of dealing with non-uniform and inhomogeneous materials, such as hygiene products, may be that one must resolve “micro-structures” and “individual components” to answer key questions. This means that the continuum approximation of materials, which is prevalent in many modelling attempts, may not provide direct information for the product/material design. This is because a typical design question is not on constitutive parameters (e.g. elastic constants, hardening/softening exponents,

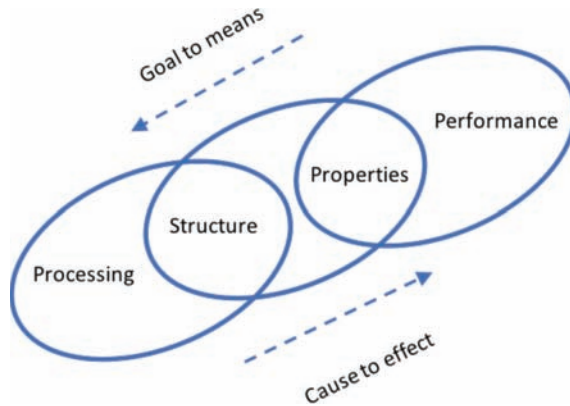


Figure 1. Product design space and two paradigms of design approach: Cause to effect and Goal to means paradigms. Adapted from [1].

etc.), but rather concrete ones, such as what kinds of micro-structures are needed to maximize softness with maintaining strength, what fibre shapes creates more fibre orientation in the thickness direction, etc. In addition, determining an appropriate constitutive law for 3D, anisotropic, nonlinear and inhomogeneous materials, such as soft papers, is still a daunting task. Another important point is robustness: product/material design requires a seamless integration of process to performance modelling (Figure 1). Most of the past attempts, however, were successful in modelling a specific subset of Figure 1 (e.g. process, structure, property or performance), but it is difficult to pass design information obtained in one subset to the other in a flexible and seamless way.

In this study, we consider soft papers as a “discrete” system, rather than a continuum, and resolve various fibre-fibre interactions and network deformations. The method we have used is one of the particle-based methods, called discrete-element method (DEM), which is robust and intuitive in representing fibres and network structures, and also in dealing with fluid- and solid-like behaviour seamlessly. It is also suited for tackling highly nonlinear problems both in static and dynamic situations (e.g. large deformation, contacts, and collisions, explosion, and fracture). Using this method, we model the processes of fibre deposition (*physical* deposition), consolidation/embossing, and creping of tissues. We also use generated fibre networks to determine tensile properties and compression properties, as they are related to softness, resilience, pliability, and structural integrity. The main goal of this study is to develop a computational design platform that will provide critical insights and understanding of material/product development, with unprecedented-level of details, based on first principles.

2. APPROACH

2.1 Computational design approach using discrete element method (DEM)

The most natural representation of materials may be a system of “particles” (like molecules). Particle is a fundamental element used in DEM, and normally (but not always) is a spherical shape. Particles interact with each other in various forms (Figure 2). For example, some particles may be bonded interacting through linear- or nonlinear-springs. Some particles collide with each other causing friction between them. All these particles may be under the influences of body forces (gravity and magnetic force). The discrete element method (DEM) originated from the studies of the flow of granular assemblies, such as sand, grain, snow, and powder [2]. Its main function is to solve the equations of motion (Newton’s second law) for *all* particles interacting each other. Original models were rather simple in terms of the types of particle-particle interactions, and are also limited in the system size (i.e. the number of particles), because of its enormous computational demand. However, with increasing computer power, as typically observed in Moore’s law, and with the equally important development of computer algorithms (e.g. contact/ neighbour search and time integration), DEM has been becoming a viable option today for analysing complex material behaviour and nonlinear dynamics. Almost in parallel to the DEM development (e.g. [23]–[28]), other particle approaches have been developed in the areas of molecular dynamics (e.g. [29]–[31]), dissipative particle dynamics and smoothed particle hydrodynamics for complex fluids and solids (e.g. [32], [33]). Today, these methods

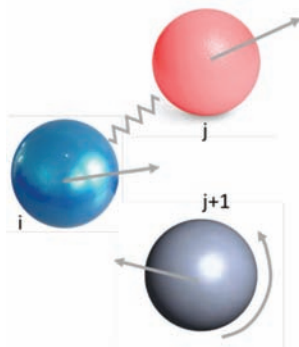


Figure 2. An example of particle interactions in discrete element method (DEM). All particles translate their positions, and also can rotate around their centre of mass. In this example, the particle i is linked to the particle j by a spring, which could be elastic, visco-elastic or plastic. The particle $j + 1$ can collide with other particles causing frictional force.

constitute a family of particle-based methods, sharing many similar numerical schemes.

The governing law of this particle system is the conservation of linear momentum and angular momentum:

$$m_i \ddot{\mathbf{r}}_i = \sum_j \mathbf{F}_{ij} + \mathbf{F}_i^b, \text{ and} \quad (1)$$

$$\frac{\partial}{\partial t} (\mathbf{I}_i \cdot \boldsymbol{\omega}_i) = \sum_j \mathbf{T}_{ij} + \mathbf{T}_i^b \quad (2)$$

where m_i and \mathbf{r}_i are a mass and position vector of the i -th particle, respectively, \mathbf{F}_{ij} is an interaction force between the i -th and j -th particles, and \mathbf{F}_i^b is a body force acting on the i -th particle. Equation (2) is the corresponding equation for angular velocity $\boldsymbol{\omega}_i$, and torques (\mathbf{T}_{ij} and \mathbf{T}_i^b) with \mathbf{I}_i the moment of inertia (tensor).

One of the advantages of DEM is that these interaction forces (and torques) can represent a large number of different materials, particularly discrete materials, by defining appropriate material-specific interactions. Accordingly, since the inception of DEM [2], there have been intensive developments in the algorithms for contact/neighbour search and time integration, and today, quite a few open-source codes are available. In this study, we have adapted an open source code, “ESyS-Particle” [3]. An important feature of this code is that it included large rotation effects of particles since the early stage of the development [4], so that, in the context of fibres, large bending and twisting deformations are correctly taken into account. Secondly, it is easy to include *clustered* particles of different shapes, which is important to represent non-spherical objects, such as fibres. Clustered particles are made by linking individual particles, and each link has 6 deformation modes, as shown in Figure 3.

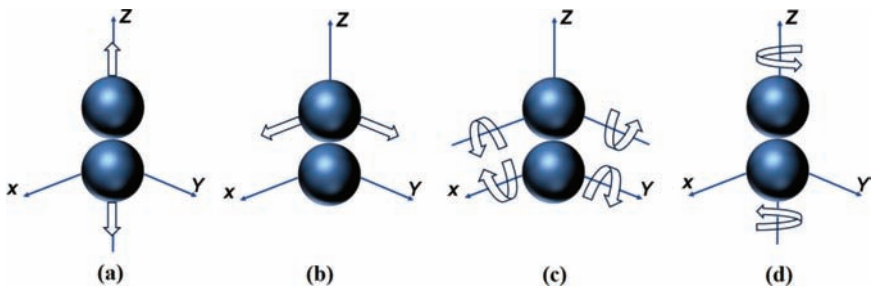


Figure 3. Deformation modes of particle link: (a) pure tension or compression, (b) shear in two tangential directions, (c) bending in two directions, and (d) twisting. Adapted from [4].

For each deformation mode of the link, a spring constant (elastic modulus) and threshold (strength) can be defined, but other constitutive laws (nonlinear and history-dependent) can also be defined by users, as we describe later. For non-linked particles, the basic interaction mode is Coulomb friction, but different interactions can also be defined to represent, for example, attraction/repulsion by long-range forces, and adhesion and liquid-bridging.

Equations (1) and (2) are solved by time integration: (1) First, apply initial conditions for positions and velocities for particles, (2) calculate all forces/toques, according to particle-particle interaction rules, (3) calculate accelerations from the forces for each particle, (3) based on the accelerations, calculate velocities and positions at the next time step for each particle, and (4) go back to Step (2) to repeat the process. For the calculation of forces and toques, one needs to detect interacting neighbour particles. This code uses Verlet list and linked cell neighbour search algorithm (e.g. [23], [27]). The time integration is made by symplectic Euler method, which is more energy-conserving than simple Euler method, with maintained computational efficiency [28].

2.2 Representation of fibres

Fibres are represented by *inter-connected particles*, such as shown in Figure 4. In order to generate curly, kinky and twisted fibres, which are common in dry

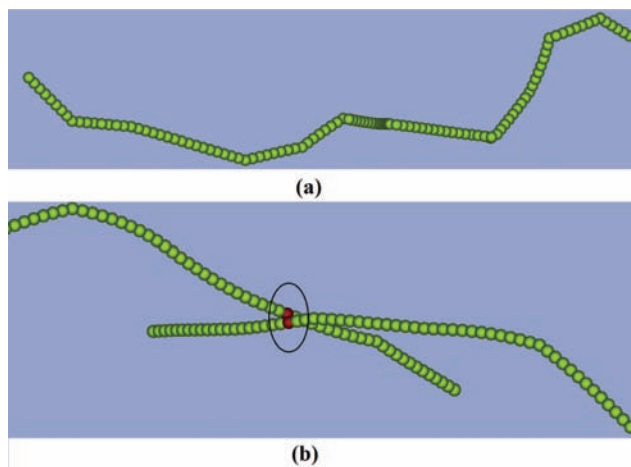


Figure 4. Representation of fibre by particles. (a) Typical fibre consisting of a series of connected particles, and (b) a fibre-fibre bond (or a fibre-fibre contact) as shown by a pair of red particles.

forming of nonwoven, we divide a fibre into a set number of linear segments. Each segment has two orientation angles: one is an angle of deviation from the previous segment, and the other is a twisting angle from the previous segment. By controlling the segment length and these two orientation angles, we can represent an arbitrary geometry of fibres [5].

Mechanical properties of single fibre may be modelled as elastic, elastic-plastic, or viscoelastic. We have implemented nonlinear-elastic-plastic case in transverse fibre property and Maxwell viscoelasticity case in fibre axial properties in ESyS code. (Note that an individual fibre deforms in the 6 deformation modes, as shown in Figure 3.) We estimated stiffness constants for tensile/compression (normal mode), shear, bending, and twisting modes from Young’s modulus and shear modulus of single fibre reported in the literature [5], [6], [7]. The corresponding threshold values, i.e. strength of single fibres, are set according to the literature [8], [9]. However, we have assumed infinite strength for the shear, bending and twisting modes for the moment, as there is currently no data available for these modes.

2.3 Representation of fibre-fibre bonds

Fibre-fibre bonds are created when two particles contact or overlap in the consolidation process. This overlap is also an important parameter that can control residual stresses/strains in the fibre-fibre bond in the wet forming process.

Mechanical properties of fibre-fibre bonds are defined in the same way as those of single fibre: there are 6 deformation modes (Figure 3), and each stiffness constant is estimated from the transverse properties of fibre in the literature [5], [10]. Fibre-fibre bonds generally fail in a mixed mode, i.e. a combination of normal, shear, bending and twisting modes. However, there is no accepted mixed-mode failure criterion and data available for fibre-fibre bonds. Therefore, we use, tentatively, a phenomenological (Hill’s type) failure criterion:

$$\frac{\max(f_r, 0)}{F_{r0}} + \frac{|f_s|}{F_{s0}} + \frac{|\tau_b|}{\Gamma_{b0}} + \frac{|\tau_t|}{\Gamma_{t0}} \geq 1 \quad (3)$$

where $f_r, f_s, \tau_b,$ and τ_t are forces and torques in normal, shear, bending and twisting modes, respectively, and $F_{r0}, F_{s0}, \Gamma_{b0},$ and Γ_{t0} are the corresponding threshold values. For $f_r < 0$ (compression), we assume there is no bond failure by the normal force. The values for F_{r0}, F_{s0} are set values to 25 mN and 5mN based on [11]. For $\Gamma_{b0},$ and $\Gamma_{t0},$ we estimated the values by assuming the bond fails in bending and twisting modes at the same strain energy as in normal and shear modes. These estimates need to be modified as more experimental data become available.

2.4 Fibre-fibre contact and interactions

Contact interactions between fibres (or even within a fibre) are modelled as a typical Coulomb-frictional interaction. However, in compression in the normal direction, we have used a nonlinear force-displacement relationship by considering the fact that the fibre cross section can collapse in compression. The experimental data of the compression of single fibres in the transverse direction (fibre collapse) [12] has been used and fit to the generalised van Wyk's equation (Matuso's equation) [13], [14]:

$$F_{ij} = C \left[\left(\frac{R_i + R_j}{\Delta_{ij}} \right)^g - 1 \right] \quad (4)$$

where F_{ij} is the interaction force (in compression) between the particles i and j , R_i and R_j are the initial radii of these particles, and Δ_{ij} is a distance between the two particles. The fitted values are $C = 0.00026$ N and $g = 3.45$.

2.5 Setting parameter values

In this paper, we present some of the key features of this design system, and some highlights of the results. For this purpose, we have defined a generic fibre and a generic fibre network structure, and have set typical parameters values, as summarised in Table 1. Unless noted otherwise, these are a default set of values for this study. Although, in this example, fibre length, fibre width and other fibre parameters are all fixed (i.e. no distribution), we normally take the data of statistical distributions of these fibre parameters in real design cases.

Table 1. Parameter values for generic fibre and generic fibre network

<i>Parameter</i>	<i>Value</i>
Fibre length	1.92 mm
Fibre diameter	32 μ m
Coarseness	(16–35) mg/100m
Fibre Young's modulus (axial direction)	10 GPa [6], [7]
Fibre shear modulus	3 GPa [6], [7]
Basis weight	20 g/m ²
Network porosity	85%
Network thickness	200 μ m
Average number of bonds per fibre	3.2 bonds
Network size in the plane	10 mm \times 10 mm

3. RESULTS AND DISCUSSIONS

3.1 Forming of fibre network

In the production of hygiene products, fibre networks are created in either dry-forming or wet-forming processes where fibres are essentially laid down on wire(s). Therefore, in order to emulate the processes (in computer), fibre networks are most commonly generated by randomly depositing fibres on a flat plane, i.e. fibres are placed on the plane (wire), “one at a time”, and the final position of the fibre is determined according to various settling rules. (The literature abounds in this area, for example, [15], [16], [17], [18].) This “mathematical deposition” is very efficient and flexible to generate fibre networks, and it captures most of the essential elements of statistical geometry of fibre network (see the review [19]). However, the recent, first-principles forming simulations also showed some subtle phenomena which are difficult to predict by the “one-fibre-at-a-time” deposition approach, for example, entanglements, 3D orientation, and density variations [20], [21]. This is due to the fact that fibres interact each other under the influences of gravity and flow field during the forming process where the fibre consistency changes continuously.

In order to retain the basic physics of the network forming and also computational efficiency, we have used a physical deposition model in 3D: the main forces applied to fibres are gravity (and/or pressure gradients) and drag forces. In this specific simulation, we have not directly included hydrodynamic effects, as we consider here an air-laid process. However, it is possible to include detailed hydrodynamic effects by coupling with SPH (smoothed particle hydrodynamics) where fluid particles are introduced to interpolate field variables in the fluid phase. Fibres are first randomly placed in space and orientation within a simulation box with a set consistency, and then start falling.

Figure 5 is a snap shot of the fibre network forming process. We have used the generic fibre source with the initial fibre consistency of 1%. (This consistency was chosen for the purpose of demonstrating the gravity deposition, but it is equally feasible to perform twin-wire forming with a realistic consistency, such as 0.1–0.15%.) We note that, with this model, effects of the initial fibre consistency are clearly seen, for example, on out-of-plane fibre orientation.

3.2 Consolidation and structuring of fibre network by TAD and embossing

After forming, the fibre network is pressed to remove water for tissues or consolidated to a desired bulk in the case of absorbent core. For tissues, the network is sometimes further subjected to through-air-drying (TAD) or to embossing to create patterned structures for bulk and softness. What is common among these

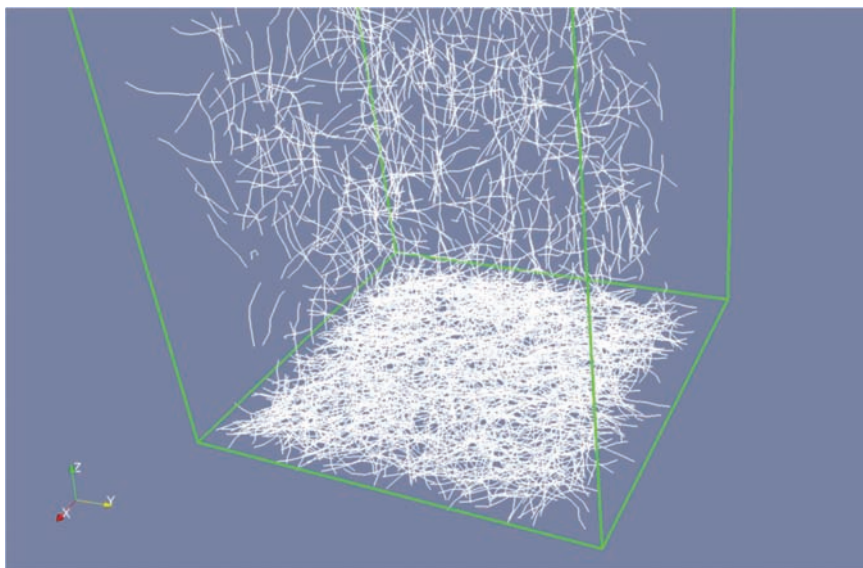


Figure 5. Forming of fibre network.

processes is that forces or displacements are applied in the thickness direction of the network, resulting in plastic deformation in fibres and thus network structures.

These processes can be easily modelled by pressing the surface either by flat or patterned surfaces (consolidation and embossing), or by applying patterned pressure-gradients on the network (TAD).

Here we have simply consolidated the structure to a set level of bulk/thickness by flat-surface compression. For patterned structuring, we will report results in a subsequent paper.

3.3 Creping

Creping is a basic operation in tissue manufacturing to add softness to base paper by generating crepe patterns and by increasing bulk. It is also known as the process that causes drastic reduction in strength properties due to the “explosion” of the sheet structure. Although, today, operational knowledge is very much established based on a large number of trials and investigations over the years, the process is still a black box in terms of what is happening on the level of fibre network. Significant efforts have been made to numerically model a creping process by considering buckling of a 1D continuum or thin film adhered on the surface of

Yankee dryer using finite element methods [35]–[39] or particle-based method [40]. Experimental approaches have also been taken by developing laboratory-scale creping equipment (e.g. [41], [42]). Among all parameter sets involved in creping, some key parameters often investigated are impacts of drying conditions and adhesive coating (e.g. [43]–[45]). The basic challenges for these numerical and experimental investigations are that the process is highly dynamic, i.e. the web hits the doctor blade, for example, at 2000 m/min, and that the destruction of 3D micro-structures of the web takes place simultaneously. DEM is ideal for investigating such a highly dynamic process on a *microscopic* level, and can provide new insights for designing fibres and tuning the process.

Figure 6 shows an example of 3D-simulation of creping. The figure captures an initial moment of creping where the base sheet hits the doctor blade at 30 m/s (1800 m/min). The base sheet originally adheres to the Yankee dryer surface with a given adhesive strength. We can see extensive destruction (or explosion) of the base sheet structure. Some fibres are broken, completely removed from the network and flies away as fibre dusts. In this figure, it is not clear to see, because of the viewing angle, but a few buckling patterns are created in the sheet, which will develop into crepe patterns. Creping patterns (frequency and amplitude) are influenced by, not only the blade angle, but also viscoelastic characteristics of the network and coating, which are, in turn, affected by its moisture content. During this process, fibre-fibre bonds are also broken. We have counted the number of broken bonds within the time period of 0.375 ms, and have found that already about 30% of the bonds are lost immediately after the explosion. This number obviously changes as a function of base sheet properties (e.g. bonding level, fibre

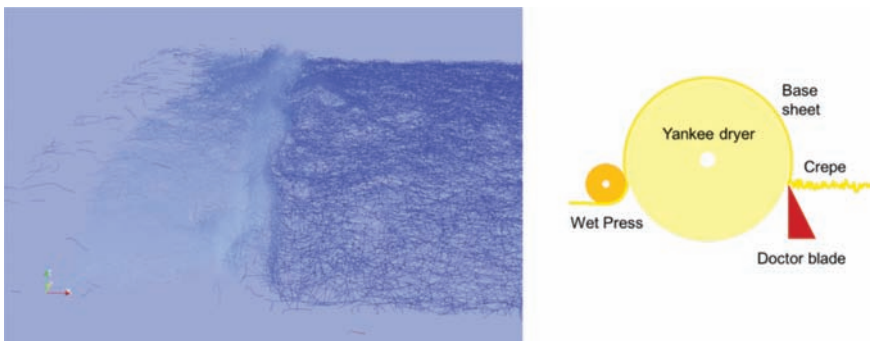


Figure 6. Example of fibre motion in creping process. The colour of fibres represents velocity magnitude (relative to the speed of Yankee dryer). The blue colour represents lower velocity and the white higher velocity. The doctor blade is not shown for the purpose of the clarity of fibre motion.

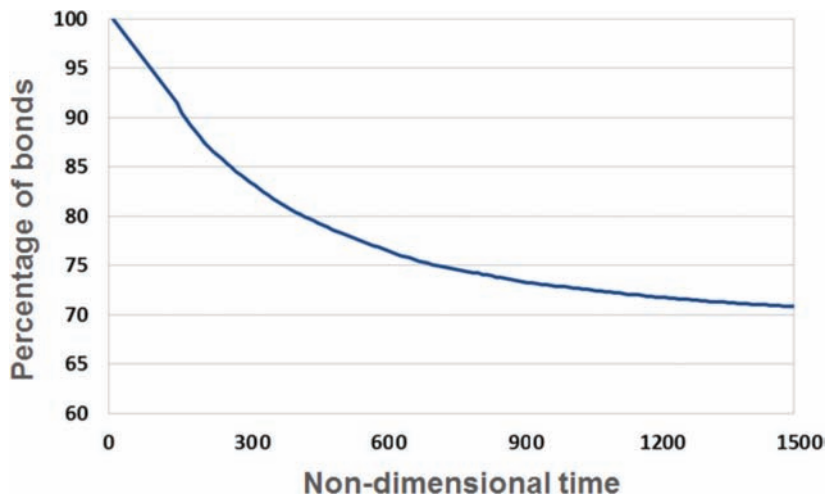


Figure 7. Change of the number of fibre-fibre bonds in the creping process. Non-dimensional time, 1500, corresponds to 0.0375 ms.

length, density, moisture content, and temperature), rheological properties of coating applied on Yankee dryer, and geometries of doctor blade. The unique feature that we found in creping simulation is that many of the above parameters are highly interactive, and a relatively small window exists for successful creping operation. With this design system, we can re-assess and further improve current operating conditions with deeper and broader understanding of creping process.

3.5 In-plane tensile testing

After generating a fibre network, we can perform various tests, both standard tests and more specialised performance tests. Here is an example of a standard tensile test (in the sheet plane direction). For low-density sheets, typical stress-strain curves are slightly nonlinear. As expected, initial elastic stiffness and ultimate strength are extremely low as compared with paper sheets of typical density, and both increase with increasing the level of fibre-fibre bonding. (We will report tensile property results in a subsequent paper.) One interesting feature of tensile properties for low density networks is that strain-energy distributions are highly non-uniform and only a small portion of fibres carries a large portion of strain energy. This *undemocratic* distribution of strain energy may be illustrated in Figure 8 (*left*), which shows a map of strain-energy stored in individual fibres. The level of strain energy is colour-coded: the red represents high strain energy, and the blue represents low. The result is understandable. As both basis weight

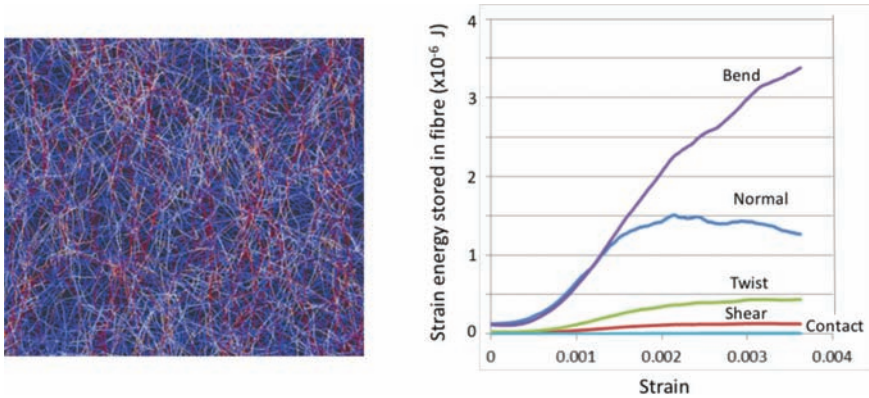


Figure 8. Distribution of strain energy stored in fibres (*left*), and the partition of strain energy into different components (*right*).

and density decreases, local variations of fibre deformation are amplified and the deformation field becomes highly non-affine. Another interesting feature of low-density networks is the mode of fibre deformation. Figure 8 (*right*) shows in which mode fibres deform during straining. Fibres deform mainly in a bending mode for low-density networks. Fibres are stretched or compressed in the fibre axial direction (“normal”), but this deformation mode is not dominating, unlike typical paper sheets of medium and high densities [11]. This intricate relationship among affine deformation, bending/stretching transition, and fibre-fibre bond density (cross-linking density) is similar to those seen in soft biopolymer networks (e.g. [22]).

3.6 Compression testing in the thickness direction

Compression of fibre network in the thickness direction is another important property. Particularly for low density networks, it is closely related to (bulk) softness, conformability and pliability. The fibre network is subjected to quasi-static compression in the thickness direction. A typical stress–strain curve is shown in Figure 9. The curve resembles typical stress–strain curves of nonwoven fibre mats [13], [14], as characterised by a very long delayed response in the initial part of the stress–strain curve and a sharp rise as the engineering strain approaches to unity. Irreversible behaviour is also shown. There are three potential sources of irreversibility in this system: the first is the breakage of fibre-fibre bonds, the second is fibre slippage (fibre rearrangement), and the third is from Maxwell’s viscoelasticity where damping by a dashpot element causes irreversible deformation. Interestingly, results

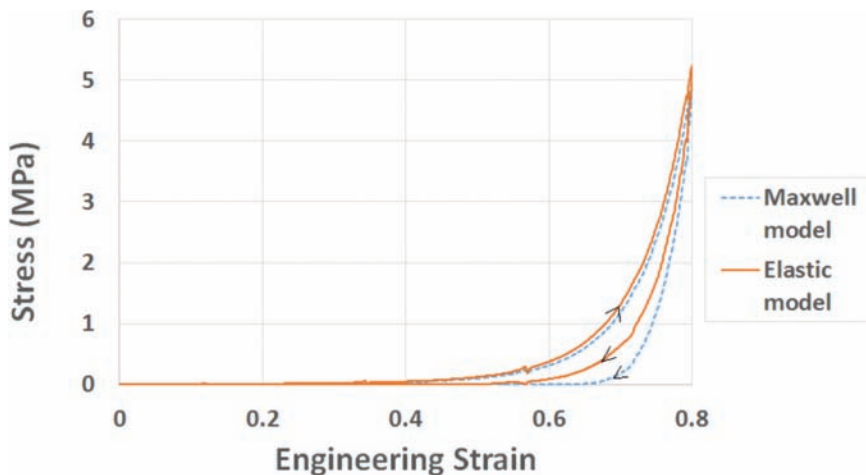


Figure 9. Compression stress-strain curve in the thickness direction.

showed that there is virtually no impact of the bond breakage on the stress-strain curve and irreversibility, though extensive breaks of fibre-fibre bonds took place [5]. However, as shown in Figure 9, the fibre slippage causes irreversible deformation, and the viscoelastic deformation of Maxwell's type also causes further irreversible deformation. It should be noted that, in compression, non-affine deformation dominates almost in the entire range of stress-strain curves [5].

4. SUMMARY AND CONCLUDING REMARKS

We have proposed particle-based methods, particularly discrete element method (DEM), as the main framework of the computational design platform for soft fibre networks of hygiene products.

Fibres are represented by a series of connected spherical particles in different lengths and geometries (curl, kinks, twists). Fibre networks are created by the deposition of those fibres under gravity, and by the subsequent consolidation under pressure. These processes have depicted the intricacies of the structures of typical low-density fibre networks in terms of the number of fibre-fibre contacts and local fibre orientations. The network is then subjected to a creping process, a critical process of tissue-making. The model was able to reproduce unique crepe frequencies as well as the destructions of the network structure. Typical tensile tests, thickness-direction compression tests, and surface softness tests are also easily performed.

As illustrated in the examples above, the method is robust in dealing with a wide range of process/material problems. It is also rather intuitive and direct to analyse the discrete structures.

The system that we have started constructing is, of course, not free from problems. A biggest challenge is accessing and interfacing the *big* material data base. There have been already huge data of material properties and structures in the literature, research institutes, universities, and companies. However, many of them are scattered, unorganised, not consistent in data format, etc., and it is not easy to access and utilise. It may require a consorted effort to create more accessible, easy-to-use big data base within the community.

Other outstanding issues are more specific to the design system. First, the current design system doesn't contain a fluid module, i.e. interfacing with fluid mechanics solver to handle problems of liquid absorption and mass transport in fibre network. In this regard, the authors' group has already another particle method, smoothed hydrodynamics (SPH) method, which is coupled with DEM, at disposal. This may be a natural handshaking between solid (DEM) and fluid (SPH). The last challenge is that DEM is still very computer intensive. For some specific problem solving, more computationally efficient methods are available. However, from the point of robustness and lower-threshold for learning (direct and intuitive), DEM has clear advantages. With continuously lowering cost of computer resources and further advancement of algorithms, this may be becoming less of an issue.

ACKNOWLEDGEMENT

The authors wish to acknowledge the financial support of the Knowledge Foundation (KK Stiftelsen) for the project, "Fibre Network Design" at the Mid Sweden University. The authors also acknowledge the discussions and insights provided by the industrial partners of the project: C. Hanson and D. Mauler of essity (formerly SCA Hygiene Products), P. Sandström, J. Bergström and K. Malmgren of SCA Forest Products AB, and G. Furman and D. Castro of NALCO Water, An Ecolab Company.

REFERENCES

1. G. B. Olson, Computational design of hierarchically structured materials. *Science* **277**(5330): 1237–1242, 1997.
2. P. A. Cundall and O. D. L. Strack. A discrete numerical model for granular assemblies. *Geotechnique* **29**(1): 47–65.D, 1979.

3. V. B. Weatherley and W. Hancock. *ESyS-Particle Tutorial and User's Guide Version 2.3.1*, Earth Systems Science Computational Centre, The University of Queensland, 2014.
4. Y. Wang. A new algorithm to model the dynamics of 3-D bonded rigid bodies with rotations, *Acta Geotechnica*, **4**(2): 117–127, 2009
5. Md. S. Hossain, P. Bergström and T. Uesaka. Nonlinear compression of fibre network: The origin of softness (to be submitted).
6. R. C. Neagu, E. K. Gamstedt and M. Lindström. Stiffness contribution of various wood fibers to composite materials, *Composite Part A: Applied Science and Manufacturing*, vol. 36, no. 6, pp.772–788, 2005.
7. R. C. Neagu, E. K. Gamstedt and F. Berthold. Influence of wood-fibre hygroexpansion on the dimensional instability of fibre mats and composites, *Journal of Composite Materials*, **40**(8): 663–699, 2006.
8. D. H. Page, F. El-Hosseiny, K. Winkler and R. Bain. The mechanical properties of single wood pulp fibres. Part I: New approach, *Pulp and Paper Magazine of Canada*, pp 72–77, 1972.
9. C. Y. Kim, D. H. Page, F. El-Hosseiny and A. P. S. Lancaster. The mechanical properties of single wood pulp fibres. Part III: The effect of drying stress on strength, *Journal of Applied Polymer Science*, **9**: 1549–1561, 1975.
10. R. E., Mark and P. P. Gillis. 'Mechanical properties of fibers,' *Handbook of Physical and Mechanical Testing of Paper and Paperboard* Vol. 1: 409–495, 1983.
11. S. Borodulina, A. Kulachenko, S. Galland and M. Nygård. Stress-strain curve of paper revisited, *Nordic Pulp and Paper Research Journal*, **27**(2): 318–328, 2012.
12. P. Wild, I. Omholt, D. Steinke and A. Schuetze. Experimental characterization of the behaviour of Wet single wood-pulp fibres under transverse compression, *Journal of Pulp and Paper Science*, **31**(3):116–120, 2005.
13. C. M. Van Wyk. Note on the compressibility of wool, *Journal of the Textile Institute Transactions*, **37**(12):T285–T292, 1946.
14. T. Komori, M. Itoh and A. Takaku. A model analysis of the compressibility of fiber assemblies, *Textile Research Journal*, **62**(10):567–574, 1992.
15. C. F. Yang. *Plane Modeling and Analysis of Fiber System*, University of Washington, 1975.
16. R. C. Hamlen. 'Paper Structure, Mechanics and Permeability: Computer Aided Modeling,' PhD Dissertation, University of Minnesota, 1991.
17. V. I. Räisänen, M. J. Alava, R. M. Nieminen and K. J. Niskanen. Elastic-plastic behaviour in fibre networks, *Nordic Pulp and Paper Research Journal*, **11**(4):243–248, 1996.
18. F. Drolet, F. and T. Uesaka. 'A stochastic structure model for predicting sheet consolidation and print uniformity,' in *Advances in Paper Science and Technology: Transactions of the 13th Fundamental Research Symposium*: 1139–1154, 2005.
19. W. Sampson. 'The structural characterisation of fibre networks in papermaking processes—A review,' in *The Science of Papermaking, Transactions of the 12th Fundamental Research Symposium, Oxford*, The Pulp and Paper Fundamental Research Society, Lancashire, UK. 2001.

20. S. B. Lindström and T. Uesaka. Particle-level simulation of forming of the fiber network in papermaking, *International Journal of Engineering Science* **46**(9): 858–876, 2008.
21. S. B. Lindstrom, T. Uesaka, T. and U. Hirn. ‘Evolution of the paper structure along the length of a twin-wire former,’ in: *Advances in Pulp and Paper*, 2009.
22. D. A. Head, A. J. Levine and F. C. MacKintosh. Distinct regimes of elastic response and deformation modes of cross-linked cytoskeletal and semiflexible polymer networks, *Physical Review E*, **68**:061907, 2003.
23. L. Verlet. Computer experiments on classical fluids. I. Thermodynamical properties of Lennard-Jones molecules, *Physical Review* **159**(1): 98, 1967.
24. J. R. Williams, and R. O’Connor. Discrete element simulation and the contact problem, *Archives of Computational Methods in Engineering* **6**(4):279–304, 1999.
25. H. P. Zhu, *et al.* Discrete particle simulation of particulate systems: A review of major applications and findings, *Chemical Engineering Science* **63**(23):5728–5770, 2008.
26. A. A. Munjiza. *The Combined Finite-Discrete Element Method*. John Wiley & Sons, 2004.
27. U. Welling, and G. Germano. Efficiency of linked cell algorithms, *Computer Physics Communications* **182**(3):611–615, 2011.
28. J. Niiranen. Fast and accurate symmetric Euler algorithm for electromechanical simulations, *IMACS*. 1999.
29. B. J. Alder, and T. Wainwright. Phase transition for a hard sphere system, *The Journal of Chemical Physics* **27**(5):1208–1209, 1957.
30. F. H. Stillinger, and A. Rahman. Molecular dynamics study of liquid water under high compression, *The Journal of Chemical Physics* **61**(12):4973–4980, 1974.
31. W. G. Hoover. Molecular dynamics, *Molecular Dynamics* **258**, 1986.
32. R. A. Gingold, and J. J. Monaghan. Smoothed particle hydrodynamics: theory and application to non-spherical stars. *Monthly Notices of the Royal Astronomical Society* **181**(3):375–389, 1977.
33. G. R. Liu, and B. Liu. *Smoothed Particle Hydrodynamics: A Mesh-Free Particle Method*. World Scientific, 2003.
34. H. Hollmark. ‘Mechanical Properties of Tissue,’ in R. E. Mark, *Handbook of Physical and Mechanical Testing of Paper and Paperboard*. New York, Marcel Dekker, 1:497–521, 1983.
35. M. K. Ramasubramanian and Z. Sun. ‘Debonding and buckling of a thin film bonded to a rigid surface,’ *ASME Applied Mechanics Division-Publications-AMD* **231**:125–138, 1998.
36. M. K. Ramasubramanian. ‘A test method for determining the shear strength of a paper-metal interface,’ *ASME Applied Mechanics Division-Publications-AMD* **209**:111, 1995.
37. M. K. Ramasubramanian and D. L. Shmagin. An experimental investigation of the creping process in low-density paper manufacturing, *Journal of Manufacturing Science and Engineering* **122**(3):576–581, 2000.
38. M. K. Ramasubramanian, Z. Sun and G. Chen. A mechanics of materials model for the creping process, *Journal of Manufacturing Science and Engineering* **133**(5):051011, 2011.

39. S. S. Gupta, 'Study of Delamination and Buckling of Paper during the Creping Process using Finite Element Method: A Cohesive Element Approach, PhD Thesis, NCSU, 2013.
40. P. Kui, A. S. Phani and S. Green. 'Particle dynamics modeling of buckle-delamination of thin film materials,' *16th International Conference of Theoretical and Applied Mechanics (ICTAM) Conference*, Montreal, Canada, 2106.
41. Jimmy Ho, *et al.* Development of a tissue creping test rig, *Chemeca, IChemEA*: 1334–1340, 2007.
42. J. Boudreau and C. Barbier. Laboratory creping equipment, *Journal of Adhesion Science and Technology* **28**(6):561–572, 2014.
43. J. H. Sloan. Yankee dryer coatings, *TAPPI J* **74**(8): 123–126, 1991.
44. M. Ryan, *et al.* Through air drying, *Drying Technology* **21**(4): 719–734, 2003.
45. B. Uner, *et al.* Adhesion interactions between poly (vinyl alcohol) and iron-oxide surfaces: The effect of acetylation, *Journal of Applied Polymer Science* **99**(6): 3528–3534, 2006.

Transcription of Discussion

COMPUTATIONAL DESIGN OF FIBRE NETWORK BY DISCRETE ELEMENT METHOD

*Shakhawath Hossain, Per Bergström,
Sohan Sarangi and Tetsu Uesaka*

Department of Chemical Engineering and FSCN, Mid Sweden University,
Sundsvall. Sweden

Tero Tuovinen University of Jyväskylä

So, it was a very nice talk. I just want to comment that if someone wants to try this discrete element method, there is very good open source environment, Kratos, with many implemented examples. And the second question is related to computational time. So in your two simulations, how much time was used to solve those and do you have some parallelization in your computations?

Tetsu Uesaka Mid Sweden University

That is a very good question, and first we used an open source code. Although after our experience I would not recommend it. The reason behind this is the accessibility of the whole, or parts of, the code is a bit complicated. There was a lot of infrastructure we had to deal with, and we were very frustrated with this complexity. So there many other open source programs that I could recommend. But for the computation time, it is a difficult to generalise, as it depends on the whole parameter set and also the type of computer you use. For example if you use your PC for the network generation it can take between 5–10 days, depending on the system size. So it depends, but that is the kind of time scale we are talking about. It is a very dynamic problem, you have to make the time-step very small and thus it takes a lot of time. (Note: we use the parallelization routinely.)

Discussion

Roger Gaudreault Invited Researcher

Thank you for this great contribution. I have two questions. Firstly, in your modelling today you only showed the fibres. Have you started to put any chemistry in your modelling at this stage?

Tetsu Uesaka

In this case, we haven't put any chemistry in. We basically took the effective property of the coating.

Roger Gaudreault

I have a related question. If you would add the chemistry, could the chemistry fluidise the fibres and make the network more uniform?

Tetsu Uesaka

Good question, but I am unable to answer these things.

Doug Coffin Miami University, Oxford OH

How do you decide on the diameter of your particle? Comparing for example, uncollapsed fibres or coarse fibres or ribbons, how do you choose the diameter?

Tetsu Uesaka

I would say, the diameter is a kind of virtual parameter. We can take fibre diameter as it is, at the same time, this diameter is used for contact detection. So in that sense, it is numerical parameter. We sometimes use it in a different way. When we talk about plastic deformation in compression we use actual fibre dimensions. If it is collapsed, we change it in the direction of compression. But at the same time, we have to recalibrate other parameters such as "I", the moment of inertia. So this is the kind of technique we use.

Artem Kulachenko KTH Royal Institute of Technology

When you consider the compressive properties of your sparse networks and when you start compressing the network in your model, it takes time before the fibres come into contact and those contacts are sufficiently loaded. Before that, the fibre bending should be dominated. It should be a bending-dominated regime. What is

important for the softness? Is it the initial response which is important or the response once in the compressed state?

Tetsu Uesaka

Yes. I think that is what we thought too, but actually the bending does not happen much even in the beginning. Maybe I can put it this way, for low basis weight, the whole compression process is one where the fibre network is perforated. Initially, the network is not connected very well, so sometimes it is actually below the stiffness perforation point. So stiffness doesn't exist initially because of that, and a finite deformation is required to see any stiffness. This is the process. So, when you look at the whole deformation process, there are actually only a few points that carry the compression load, which happen to be the connected chains of the contacts. It's an amazing property.

Ron Peerlings

I have a question that is related to Doug's. You digitized the fibre by a number of these particles. If you would change that number, so along the fibre you have more or fewer, does that have an effect on the results?

Tetsu Uesaka

That is a good question. We can separate and penetrate the particles with each other, then we have to have a contact algorithm to handle it and that is what we did. In all the deformations, the tensile load is not that much a problem. That is a very intense deformation in the small scale, but we haven't checked that point in the case of creep. As you can see, the length scale of the stress waves is very small, in the same order of fibre width.

Doug Coffin Miami University, Oxford, OH

I have one more question. So, on the 'boring' tensile test if we load it and then unload it and reload for tissue paper, the second response is much different because I would imagine that the energy is being shifted from bending to in-plane. Can your model predict that?

Tetsu Uesaka

Yes, we can. In the tension test the deformation mode is from bending to stretching, and when unloaded, this deformation mechanism is partly recovered, but still shows irreversible deformations.

Discussion

Doug Coffin

Right, but also the bending is inelastic, in fact I would say that it's permanent. Is that in your model?

Tetsu Uesaka

Yes, the model we presented here for the tensile test is an elastic-failure model.